

Dispersion corrections to parity violating electron scattering

M. Gorchtein*, C. J. Horowitz* and M. J. Ramsey-Musolf[†]

**Nuclear Theory Center, Indiana University, Bloomington, IN 47408, USA*

[†]*University of Wisconsin-Madison, Madison, WI 53706, USA*

Abstract. We consider the dispersion correction to elastic parity violating electron-proton scattering due to γZ exchange. In a recent publication, this correction was reported to be substantially larger than the previous estimates. In this paper, we study the dispersion correction in greater detail. We confirm the size of the dispersion correction to be $\sim 6\%$ for the QWEAK experiment designed to measure the proton weak charge. We enumerate parameters that have to be constrained to better than relative 30% in order to keep the theoretical uncertainty for QWEAK under control.

Keywords: QWEAK, dispersion relations

PACS: 12.15.Lk, 11.55.Fv, 12.40.Nn, 13.60.Fz

Precision tests of the Standard Model at low energies provide an important framework for New Physics searches and for setting stringent constraints on the parameters of possible extensions of the Standard Model (SM). Such tests involve high precision measurements of parameters that are suppressed or precisely vanish in SM. An important example of such parameter is the weak charge of the proton, $Q_W^p = 1 - 4 \sin^2 \theta_W$. With the value of the weak mixing angle at low momentum transfers $\sin^2 \theta_W(0) = 0.23807 \pm 0.00017$ [1], the SM predicts the proton weak charge of order ≈ 0.05 . A precise 4% (combined 2% experimental and 2% theoretical uncertainties) determination of the weak charge of the proton is the aim of the QWEAK experiment at Jefferson Lab [2]. In this experiment, parity violating asymmetry in polarized electron scattering $A_{PV} = (\sigma_R - \sigma_L)/(\sigma_R + \sigma_L)$ will be measured, $\sigma_R(\sigma_L)$ standing for the differential cross section in elastic electron-proton scattering with the incidental electron beam spin parallel (antiparallel) to its direction, respectively. To leading order in the momentum transfer t and in Fermi constant, the parity violating asymmetry arises from the interference of parity conserving and parity violating amplitudes at tree level. Including radiative corrections of order α , one has

$$A^{PV} = \frac{G_F t}{4\pi\alpha\sqrt{2}} Q_W^p [1 + \text{Re}\delta_{RC} + \text{Re}\delta_{\gamma Z}(v)] + \mathcal{O}(t^2), \quad (1)$$

Above, we denote all the radiative corrections except the γZ direct and crossed boxes by δ_{RC} , and we explicitly indicate that the dispersion correction $\delta_{\gamma Z}$ is function of energy v . The corrections δ_{RC} were considered in various works, to mention the most important references [1, 3], and the combined theoretical uncertainty associated with these was shown not to exceed 2.2%. The dispersion correction $\delta_{\gamma Z}$ is the only one that can obtain a sizeable contribution from hadronic structure. In [4], the dispersion correction was

represented as the sum $\delta_{\gamma Z} = \delta_{\gamma Z_A} + \delta_{\gamma Z_V}$, and two forward sum rules were established,

$$\text{Re}\delta_{\gamma Z_A}(\nu) = \frac{2\nu}{\pi} \int_{\nu_\pi}^\infty \frac{d\nu'}{\nu'^2 - \nu^2} \text{Im}\delta_{\gamma Z_A}(\nu'), \quad (2)$$

$$\text{Re}\delta_{\gamma Z_V}(\nu) = \frac{2}{\pi} \int_{\nu_\pi}^\infty \frac{\nu' d\nu'}{\nu'^2 - \nu^2} \text{Im}\delta_{\gamma Z_V}(\nu'), \quad (3)$$

The respective imaginary parts can be expressed as integrals over the PV DIS structure functions $\tilde{F}_i(x, Q^2)$,

$$\begin{aligned} \text{Im}\delta_{\gamma Z_A}(\nu) &= \frac{\alpha}{2Q_W^p} g_A^e \int_{W_\pi^2}^s \frac{dW^2}{(s - M^2)^2} \int_0^{Q_{max}^2} \frac{dQ^2}{1 + \frac{Q^2}{M_Z^2}} \left[\tilde{F}_1 + \left(\frac{2Pk_1Pk}{PqQ^2} - \frac{P^2}{2Pq} \right) \tilde{F}_2 \right] \\ \text{Im}\delta_{\gamma Z_V}(\nu) &= -\frac{\alpha}{2Q_W^p} g_V^e \int_{W_\pi^2}^s \frac{dW^2}{(s - M^2)^2} \int_0^{Q_{max}^2} \frac{dQ^2}{1 + \frac{Q^2}{M_Z^2}} \frac{(P, k + k_1)}{2(Pq)} \tilde{F}_3 \end{aligned} \quad (4)$$

with $W_\pi^2 = (M + m_\pi)^2$ the pion production threshold, and $Q_{max}^2 = \frac{(s - M^2)(s - W^2)}{s}$. The sum rules of Eqs. (2,3) are new results. In the past, only their values at $\nu = 0$ were calculated in the framework of atomic PV. Due to the explicit factor of ν , the correction $\delta_{\gamma Z_A}$ is exactly zero for zero energy, in accordance with [3], and has been neglected in the literature even for non-zero energies. The dispersion relation calculation of [4] lead to $\delta_{\gamma Z_A} \sim 6\%$ that should be compared with zero in the analysis of the QWEAK experiment. The correction $\delta_{\gamma Z_V}$ obtains its value due to hard kinematics inside the loop and is largely energy-independent [3, 5]. In the rest of this article, we concentrate on $\delta_{\gamma Z_A}$ only. The sum rule of Eq. (2) itself is model-independent; however, in absence of any detailed PVDIS data, the input in this sum rule will depend on a model. We proceed by modeling the electromagnetic data first.

MODELING REAL AND VIRTUAL PHOTOABSORPTION DATA

We will use the following three models to model the electromagnetic DIS structure functions F_i :

- **Model I:** The model used in [4] utilized the resonance parameters obtained in [6] and the non-resonant Regge contribution from [7] that was fitted to the real photon data at high energies. Ref. [7] also provides the Q^2 -dependence of the high-energy part, so no additional modelling was necessary here. For the estimates of [4], a simple dipole model with the dipole mass $\Lambda \approx 1$ GeV for all the transition resonance form factors was employed.
- **Model II:** Another form of resonance and background contributions and transition form factors was used in [15] to fit virtual photon data.
- **Model III:** As Fig. 1 clearly demonstrates, the background of [15] cannot be used too far beyond the resonance region. Therefore, we opt for Model III that uses the background from Model I, and adopt the resonance contribution from Model II.

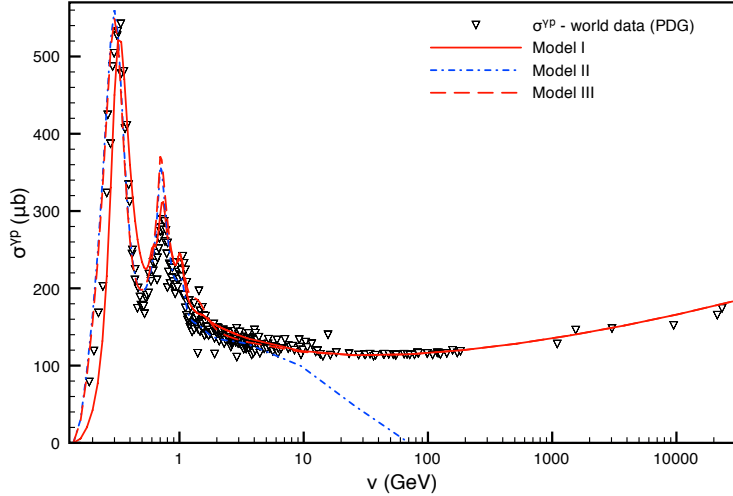


FIGURE 1. World data on total photoabsorption [8, 9, 10, 11, 12, 13] (see [14] for the complete list) compared to the three models described in the text.

In Figs. 1 and 2, we display the comparison of the three models with the data for the differential cross section for inclusive electroproduction in the resonance region. The Model I [4] is shown by solid red lines, Model II by the solid blue line, and Model III is represented by a long-dash red line. From Fig. 2 it becomes clear that Model I largely underestimates the JLab data in the whole resonance region, apart from the real photon point Fig. 1. Model III also provides a very good description of the DIS data for $F_2(x, Q^2)$ at low and moderate values of Q^2 [7].

ISOSPIN STRUCTURE

Once the parameters are fixed, we can employ simple isospin considerations for each contribution. Note that because breaking down the experimental data into the sum of resonances and background is a model-dependent procedure, also the isospin rotation is only defined within a given model. For the $N \rightarrow N^*(I = 1/2)$ transition, the isospin decomposition resembles that for the elastic form factors, $\langle N^* | J_{NC,V}^\mu | p \rangle = (1 - 4s^2\theta_W) \langle N^* | J_{em}^\mu | p \rangle - \langle N^* | J_{em}^\mu | n \rangle$. It is then straightforward to relate the contribution of a resonance R with isospin $1/2$ to the interference γZ "cross section", to its contribution to the electromagnetic cross section by introducing the isospin scaling factors

$$\xi_{Z/\gamma}^R \equiv \frac{\sigma_{T,R}^{\gamma Z,p}}{\sigma_{T,R}^{\gamma\gamma p}} = (1 - 4s^2\theta_W) - \frac{A_{R,1/2}^p A_{R,1/2}^{n*} + A_{R,3/2}^p A_{R,3/2}^{n*}}{|A_{R,1/2}^p|^2 + |A_{R,3/2}^p|^2} \quad (5)$$

Above, $A_{R,1/2(3/2)}^{p(n)}$ are the transition helicity amplitudes for exciting the resonance R on the proton (neutron), respectively, whereas $\sigma_{T,R}$ denotes the contribution of the resonance R to the transverse virtual photon cross section. The scaling factors $\xi_{Z/\gamma}^R$

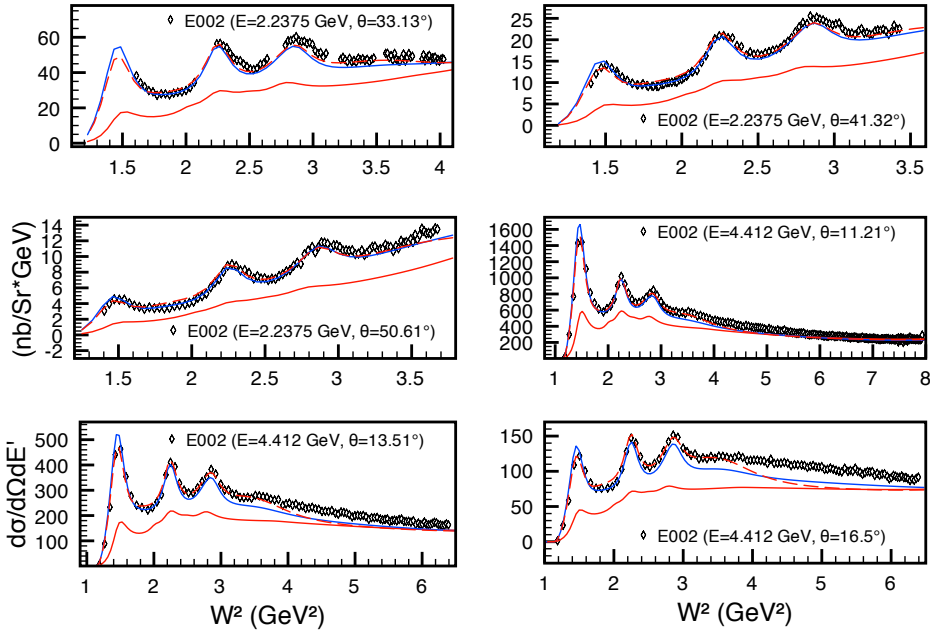


FIGURE 2. Differential cross section data in the resonance region from JLab E002 [16] are shown in comparison with the three models.

depend both on the relative size and relative phase of the transition amplitude on the proton and on the neutron. To obtain both, we use the results of the constituent quark model of Ref. [18] for the transition helicity amplitudes. For isovector transitions $N \rightarrow \Delta(\Delta^*)$, the scaling factor in the SM is $\xi_{Z/\gamma}^{\Delta} = 2(1 - 2\sin^2 \theta_W)$. Vector Meson Dominance Model (VDM) capitalizes on the fact that the photon (Z-boson) has the same quantum numbers as vector mesons and can be represented as a superposition of a few vector mesons, $|\gamma\rangle = \sum_{V=\rho,\omega,\phi,\dots} |V\rangle$. In the naive VDM, these three channels cannot mix among each other, and one obtains a prediction for the ratios of the cross sections of ρ , ω , ϕ production, $\sigma^{\gamma^* p \rightarrow \rho p} : \sigma^{\gamma^* p \rightarrow \omega p} : \sigma^{\gamma^* p \rightarrow \phi p} = 1 : (q^{I=0}/q^{I=1})^2 : (q^s/q^{I=1})^2 = 1 : 1/9 : 2/9$, where we defined $q^{I=0} = 1/(3\sqrt{2})$, $q^{I=1} = 1/\sqrt{2}$ and $q^s = -1/3$. The above predictions were confronted to the experimental data at high energies and for Q^2 that ranged from zero to several GeV^2 [19] and showed a very good agreement for the ω/ρ ratio, while for the ϕ/ρ ratio the agreement was not as good. Accommodating these considerations here, we obtain the following ratio of the high energy non-resonant (NR) contributions to $\gamma^* p \rightarrow Zp$ and $\gamma^* p \rightarrow \gamma^* p$ cross sections:

$$\xi_{Z/\gamma}^{NR} \approx \frac{g_V^{I=1} q^{I=1} + g_V^{I=0} q^{I=0} + g_V^s q^s}{(q^{I=1})^2 + (q^{I=0})^2 + (q^s)^2} = 2(1 - 4\sin^2 \theta_W) \quad (6)$$

where we make use of the SM definition $g_V^{I=0} = -4\sin^2 \theta_W/(3\sqrt{2})$, $q^{I=1} = (2 - 4\sin^2 \theta_W)/\sqrt{2}$ and $q^s = -1 + 4\sin^2 \theta_W/3$. We summarize these results in Table 1.

TABLE 1. Isospin scaling factors $\xi_{Z/\gamma}$ for resonances and non-resonant (NR) background.

$P_{33}(1232)$	$S_{11}(1535)$	$D_{13}(1520)$	$S_{11}(1665)$	$F_{15}(1680)$	$P_{11}(1440)$	$F_{37}(1950)$	NR
1.075	0.885	0.938	0.473	0.35	0.745	1.075	1.075

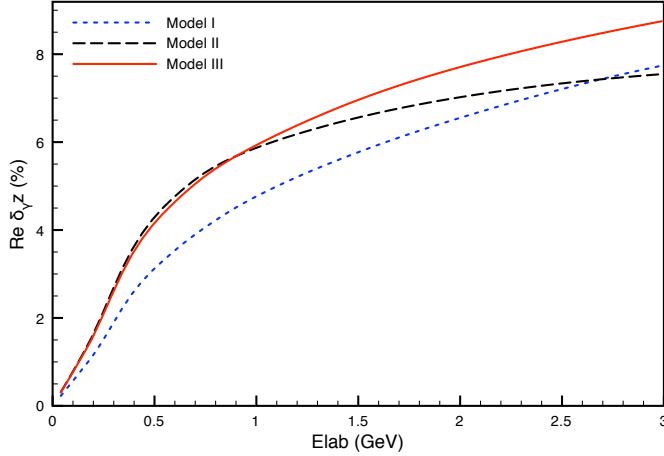


FIGURE 3. Results for the dispersion correction as calculated in the Models I, II and III.

RESULTS FOR $\text{Re } \delta_{\gamma Z_A}$

Fig. 3 shows the energy dependence of $\text{Re } \delta_{\gamma Z_A}$, calculated in three different models. The individual contributions at QWEAK energy are shown in Table 2. We next discuss the size and origin of the uncertainty in calculating $\text{Re } \delta_{\gamma Z_A}$. It comes about from i) modeling the electromagnetic data, and ii) from the respective isospin structure. To estimate the former, we average over the three models discussed above and displayed in Fig. 3, leading to $\text{Re } \delta_{\gamma Z_A} = (5.85 \pm 0.45)\%$, with most of the error bar due to the Model I. Because the latter underestimates the experimental data throughout the resonance region for non-zero Q^2 , it is clear that this estimate represents an upper bound for the model dependence. In an upcoming work, we plan to directly fit the parameters of Model III to the data that will allow to significantly reduce the model-dependent error, given the quality of the experimental data shown in Figs. 1, 2. The isospin structure represents a more significant source of uncertainty. We will next indicate, to what precision the isospin scaling factors of Table 1 should be constrained to keep the uncertainty of $\text{Re } \delta_{\gamma Z_A}$ under control. From Table 2, it is seen that contributions of $D_{13}(1520)$, $F_{15}(1680)$,

TABLE 2. Individual resonances and background (NR) contributions to the dispersion correction $\text{Re } \delta_{\gamma Z_A}$ for QWEAK energy $E_{lab} = 1.165$ GeV. Results of Model III are quoted.

$P_{33}(1232)$	$S_{11}(1535)$	$D_{13}(1520)$	$F_{15}(1680)$	$S_{11}(1665)$	$P_{11}(1440)$	$F_{37}(1950)$	NR
1.27 %	0.44 %	0.21 %	0.06 %	0.05 %	0.10 %	0.50 %	3.61 %

$S_{11}(1665)$ and $P_{11}(1440)$ resonances have very little impact on the size of the dispersion correction. We can therefore afford to assign a conservative uncertainty of 50% to each. $P_{33}(1232)$ has been studied in many phenomenological models, and we believe that it is realistic to constrain the scaling factor $\xi_{Z/\gamma}^{P_{33}(1232)}$ to better than 20% that would translate into 0.25% for the dispersion correction. For $S_{11}(1535)$, the isospin structure might be more complex, since it couples strongly to $\pi\pi N$ states along with πN , but the absolute size of the correction quoted in Table 2 allows for a larger relative uncertainty here. Constraining $\xi_{Z/\gamma}^{S_{11}(1535)}$ to relative 30% would lead to 0.13% for $\delta_{\gamma Z}$. Finally, we turn to the uncertainties associated with the higher energy contributions. It has to be mentioned that the contribution associated in [15] with a resonance around $W = 1950$ MeV cannot be ultimately identified with the $F_{37}(1950)$ state listed in PDG [14]. This contribution may represent a missing strength of the background at $W \geq 1900$ MeV that can be seen in the two lower panels of Fig. 2, rather than a real resonance. Constraining this contribution to relative 50% means 0.25% for $\delta_{\gamma Z}$. For the background, we assign the 100% uncertainty to the strange quarks contribution to the scaling factor in Eq. (6), $\xi_{Z/\gamma}^{NR} = 1.075(1 \pm 0.34)$. Putting the above discussion together, we write

$$\text{Re } \delta_{\gamma Z}(v = 1.165 \text{ GeV}) = (5.85 \pm 0.45_{\text{mod}} \pm 1.23_{\text{iso}})\%. \quad (7)$$

We conclude that the main uncertainty to the dispersion correction comes from the isospin decomposition of the electromagnetic data, most notably from high energy background. We showed how the total uncertainty can be represented as an uncertainty in the four isospin scaling parameters, $\xi_{Z/\gamma}^{NR}$, $\xi_{Z/\gamma}^{P_{33}(1232)}$, $\xi_{Z/\gamma}^{S_{11}(1535)}$ and $\xi_{Z/\gamma}^{F_{37}(1950)}$. The estimates of uncertainties in these factors that we presented are only approximate, and will be studied in greater detail in an upcoming work in order to ensure the interpretability of the QWEAK experiment.

REFERENCES

1. J. Erler, M.J. Ramsey-Musolf, Phys. Rev. **D 72** (2005), 073003.
2. W.T.H. Van Oers [QWEAK Collaboration], Nucl. Phys. **A 790** (2007), 81.
3. W.J. Marciano, A. Sirlin, Phys. Rev. **D 27** (1983), 552; *ibid.* **D 29** (1984), 75; *ibid.* **D 31** (1985), 213.
4. M. Gorchtein, C.J. Horowitz, Phys. Rev. Lett. **102** (2009), 091806.
5. M.J. Ramsey-Musolf, Phys. Rev. **C 60** (1999), 015501.
6. N. Bianchi *et al.*, Phys. Rev. **C 54** (1996), 1688.
7. G. Cvetic, D. Schildknecht, B. Surrow, M. Tentyukov, Eur. Phys. J. **C 20** (2001), 77.
8. E.D. Bloom *et al.*, SLAC-PUB-0653 (1969).
9. T.A. Armstrong *et al.*, Phys. Rev. **D 5** (1972), 1640.
10. D.O. Caldwell *et al.*, Phys. Rev. **D 7** (1973), 1362.
11. D.O. Caldwell *et al.*, Phys. Rev. Lett. **40** (1978), 1222.
12. S. Chekanov *et al.* [ZEUS Collaboration], Nucl. Phys. **B 627** (2002), 3.
13. G.M. Vereshkov *et al.*, Phys. Atom. Nucl. **66** (2003), 565.
14. C. Amsler *et al.*, Phys. Lett. **B 667** (2008), 1.
15. M.E. Christy, P.E. Bosted, [arXiv:0712.3731 hep-ph]
16. Preliminary results from JLab E00-002, C. Keppel, M.I. Niculescu, *private communication*.
17. J. Breitweg *et al.* [ZEUS Collaboration], Eur. Phys. J. **C 7** (1999), 609.
18. R. Koniuk, N. Isgur, Phys. Rev. **D 21** (1980), 1868.
19. J. Breitweg *et al.* [ZEUS Collaboration], Phys. Lett. **B 487** (2000), 273.